Absolute optical instruments without spherical symmetry

Tomáš Tyc[1], H. L. Dao[2], and Aaron J. Danner[2]
[1]*Department of Theoretical Physics and Astrophysics, Masaryk University, Kotlářská 2, 61137 Brno, Czech Republic*
[2]*Department of Electrical and Computer Engineering, National University of Singapore, 4 Engineering Drive 3, 117583 Singapore*
(Dated: June 27, 2015)

ABSTRACT

Until now, the known set of absolute optical instruments has been limited to those containing high levels of symmetry. Here, we demonstrate a method of mathematically constructing refractive index profiles that result in asymmetric absolute optical instruments. The method is based on the analogy between geometrical optics and classical mechanics and employs Lagrangians that separate in Cartesian coordinates. In addition, our method can be used to construct the index profiles of most previously known absolute optical instruments, as well as infinitely many new ones.

I. INTRODUCTION

An absolute instrument (AI) is an optical device that images a region of space stigmatically, i.e., without any aberrations [1, 2]. The first non-trivial AI known as Maxwell's fish eye was discovered by J. C. Maxwell in 1854 [3]. However, for a very long time the set of known AIs remained extremely limited, the other known example of an AI then being a plane mirror. This changed in 2006 when J. C. Miñano pointed out that several previously known devices such as Eaton or Luneburg lenses are in fact AIs, and discovered several new ones [4]. Later in 2011 T. Tyc *et al.* presented a very general method of designing refractive index profiles of AIs that can easily generate uncountably many AIs [2].

All of these AIs, however, have spherically (in case of a three-dimensional, 3D, AI) or rotationally (in the 2D case) symmetric refractive index profiles. It was not clear until very recently whether AIs without this symmetry exist at all. The answer to this question turned out to be positive in the work of A. Danner *et al.* who discovered a new class of AIs called Lissajous lenses in which rays form Lissajous curves [5]. However, whether other AIs without spherical or rotational symmetry exist or not (other than conformal maps of lenses with such symmetry) was still not clear.

In this paper, we show that the answer to this question is also positive, and we present a new class of AIs that are generalisations of the previously found Lissajous lenses. The class of these lenses is very rich and their main feature is that the Lagrangian for the corresponding mechanical problem separates in Cartesian coordinates. We demonstrate their imaging properties both for light rays and waves and present a number of examples.

II. CONSTRUCTION OF THE LENS

Similarly as in [5], we take advantage of the analogy between classical mechanics and geometrical optics [6] for constructing the lens. This analogy comes from the similarity between Fermat's principle in optics [1] and the Maupertuis principle in mechanics [7] and its consequence is that the trajectories of a particle with the Lagrangian $L = v^2/2 - U(\vec{r})$ (we set the mass to unity) and energy E have the same geometrical shapes as light rays in a medium with refractive index

$$n(\vec{r}) = \sqrt{2[E - U(\vec{r})]}\,. \tag{1}$$

We will first design the potential $U(\vec{r})$ that gives closed trajectories for the mechanical problem and then proceed to the optical case. To do this, we will consider first just a 2D problem and assume that the potential $U(\vec{r})$ separates in Cartesian coordinates, $U(\vec{r}) = U_x(x) + U_y(y)$. We will also assume without loss of generality that both potentials U_x, U_y have a global minimum $U_x(0) = U_y(0) = 0$. The Lagrangian

$$L = \frac{\dot{x}^2 + \dot{y}^2}{2} - U_x(x) - U_y(y) \tag{2}$$

then completely separates and yields two conservation laws for the energies corresponding to motions in the x and y directions that sum to the total energy E:

$$\frac{\dot{x}^2}{2} + U_x(x) = E_x, \quad \frac{\dot{y}^2}{2} + U_y(y) = E_y, \quad E_x + E_y = E\,. \tag{3}$$

For each energy E_x, the motion in the x direction is limited to the interval between turning points $x_1(E_x)$ and $x_2(E_x)$, $x_1(E_x) \le 0 \le x_2(E_x)$, at which $U_x = E_x$. Using Eq. (3), we can easily calculate the period of oscillation in the x direction corresponding to motion from $x_1(E_x)$ to $x_2(E_x)$ and back:

$$T_x(E_x) = 2\int_{x_1(E_x)}^{x_2(E_x)} \frac{\mathrm{d}x}{\sqrt{2[E_x - U_x(x)]}}\,. \tag{4}$$

In a similar way we can express the period of oscillation $T_y(E_y)$ in the y direction in terms of $U_y(y)$ and $E_y = E - E_x$. Obviously, if the ratio of the periods $T_x(E_x)$ and $T_y(E - E_x)$ is rational for some energy E_x, the motion of the particle will be periodic and the trajectory will be closed.

Suppose now that we vary the energies E_x and E_y, keeping their sum E fixed. This in general changes both the periods T_x and T_y. However, if the potentials U_x and U_y are designed such that the ratio T_x/T_y remains rational for all $E_x \in [0, E]$, then the motion will be periodic and we still obtain closed trajectories. This way, all the trajectories of the particle with the total energy E will be closed. For the same reason all light rays in the corresponding refractive index profile (1) will be closed and we arrive at an absolute optical instrument. The simplest way to achieve this is to keep the ratio constant and equal to $k \in \mathbb{Q}$:

$$T_y(E_y) = T_y(E - E_x) = kT_x(E_x) = kT_x(E - E_y)\,, \qquad 0 \le E_x \le E\,. \tag{5}$$

To proceed with designing the potentials U_x and U_y, we employ the procedure that enables us to invert Eq. (4) and find the potential U_x if the period is known as a function of energy, $T_x(E_x)$. This procedure is described in [7] and it is closely related to deriving the inverse Abel transformation. The result is

$$\Delta x(U_x) \equiv x_2(U_x) - x_1(U_x) = \frac{1}{\pi\sqrt{2}} \int_0^{U_x} \frac{T_x(E_x)\mathrm{d}E_x}{\sqrt{U_x - E_x}}\,. \tag{6}$$

Here we write the turning points as $x_{1,2}(U_x)$ instead of $x_{1,2}(E_x)$. This expresses the fact that $x_{1,2}(U_x)$ can be understood as functions that are inverse to the two branches of the potential $U_x(x)$ for $x \le 0$ and $x \ge 0$, respectively. Eq. (6) does not determine the potential uniquely, but there is still a lot of freedom; one can, e.g., choose the function $x_1(U_x)$ and use Eq. (6) to get $x_2(U_x)$. The only restrictions are that $x_1(U_x)$ and $x_2(U_x)$ must be non-increasing and non-decreasing, respectively, such that $U_x(x)$ can be reconstructed by inverting them. One possible choice corresponds to the requirement that the potential should be symmetric; in that case $x_2(U_x) = -x_1(U_x) = \Delta x(U_x)/2$. As we will see, this freedom can be employed for greatly enlarging the set of possible absolute instruments. Formulas analogous to Eqs. (4) and (6) hold also for the motion in the y direction.

Eqs. (6) and (5) can be used for designing new 2D absolute instruments. Moreover, this can be done in two different ways that we discuss separately below.

II.1. Choosing $T_x(E_x)$ and k, and calculating $U_x(x)$ and $U_y(y)$

One way of finding the potentials U_x and U_y is to choose k and the function $T_x(E_x)$. The potential U_x can then be found with the help of Eq. (6) (including the above mentioned freedom), and the potential U_y can be found with the y-version of Eq. (6) using $T_y(E_y) = kT_x(E - E_y)$. The only thing one has to bear in mind is that the function $T_x(E_x)$ cannot be chosen completely arbitrarily, but it must be such that the resulting $\Delta x(U_x)$ and $\Delta y(U_y)$ are non-decreasing functions, otherwise the potentials U_x and/or U_y could not be defined.

II.2. Choosing $U_x(x)$ and k, and calculating $U_y(y)$

Another way of designing AIs is to choose the constant k and the potential $U_x(x)$. We can then calculate $T_x(E_x)$ using Eq. (4) and find U_y using Eq. (5) together with the y-version of Eq. (6). When we put everything together, we get for $\Delta y(U_y)$

$$\Delta y(U_y) = \frac{1}{\pi\sqrt{2}} \int_0^{U_y} \frac{T_y(E_y)\,\mathrm{d}E_y}{\sqrt{U_y - E_y}}$$
$$= \frac{1}{\pi\sqrt{2}} \int_0^{U_y} \frac{kT_x(E - E_y)\,\mathrm{d}E_y}{\sqrt{U_y - E_y}} \tag{7}$$
$$= \frac{1}{\pi} \int_0^{U_y} \int_{x_1(E-E_y)}^{x_2(E-E_y)} \frac{k\,\mathrm{d}x}{\sqrt{U_y - E_y}\sqrt{E - E_y - U_x(x)}}\,\mathrm{d}E_y\,. \tag{8}$$

To proceed with calculation, we have to change the integration variable in the inner integral from x to U_x. This has to be done separately for the two branches $x_1(U_x)$ and $x_2(U_x)$. For this purpose, we write in general the integral

$$\int_{x_1(E-E_y)}^{x_2(E-E_y)} \mathrm{d}x = \int_{x_1(E-E_y)}^{0} \mathrm{d}x + \int_0^{x_2(E-E_y)} \mathrm{d}x \tag{9}$$
$$= \int_{E-E_y}^{0} \frac{\mathrm{d}x_1}{\mathrm{d}U_x}\,\mathrm{d}U_x + \int_0^{E-E_y} \frac{\mathrm{d}x_2}{\mathrm{d}U_x}\,\mathrm{d}U_x$$
$$= \int_0^{E-E_y} \frac{\mathrm{d}\Delta x}{\mathrm{d}U_x}\,\mathrm{d}U_x\,. \tag{10}$$

Using this in Eq. (8), we get

$$\Delta y(U_y) = \frac{k}{\pi} \int_0^{U_y} \mathrm{d}E_y \times \int_0^{E-E_y} \frac{\mathrm{d}\Delta x}{\mathrm{d}U_x} \frac{\mathrm{d}U_x}{\sqrt{E - E_y - U_x}\sqrt{U_y - E_y}}\,. \tag{11}$$

The calculation of the above double integral is shown in the Appendix. The result is

$$\Delta y(U_y) = \frac{2k}{\pi} \int_0^{E} \frac{\mathrm{d}\Delta x(U_x)}{\mathrm{d}U_x} \ln\left(\frac{\sqrt{U_y} + \sqrt{E - U_x}}{\sqrt{|E - U_x - U_y|}}\right) \mathrm{d}U_x \tag{12}$$
$$= \frac{2k}{\pi} \int_{x_1(E)}^{x_2(E)} \ln\left(\frac{\sqrt{U_y} + \sqrt{E - U_x(x)}}{\sqrt{|E - U_x(x) - U_y|}}\right) \mathrm{d}x\,. \tag{13}$$

Here we have written the result in two equivalent forms expressed as an integral over U_x or x, respectively.

From the $\Delta y(U_y)$ calculated with the help of Eq. (12) we can then find an infinite number of potentials $U_y(y)$ employing the freedom discussed below Eq. (6). If we require that U_y is symmetric, then the solution is unique.

Summing up, our method works by generating pairs of potentials $U_x(x)$, $U_y(y)$ which yield independent motion of the particle in the x and y directions. No matter how the energy is distributed between the two degrees of freedom, the ratio of time periods corresponding to motion in these two directions is rational. This yields periodic motion and hence closed trajectories. We can then design the refractive index (6) that will yield closed ray trajectories. In this way we obtain a plethora of 2D absolute instruments without rotational symmetry.

III. EXAMPLES

We will illustrate our method on several examples.

III.1. Lissajous lens

If we choose $T_x(E_x) = T = \text{const.}$ and require both potentials U_x, U_y to be symmetric, we get from Eq. (6) $\Delta x(U_x) = T\sqrt{2U_x}/\pi$, $\Delta y(U_y) = kT\sqrt{2U_y}/\pi$ and consequently

$$U_x(x) = \frac{1}{2}\left(\frac{2\pi}{T}\right)^2 x^2\,, \qquad U_y(y) = \frac{1}{2}\left(\frac{2\pi}{kT}\right)^2 y^2\,. \tag{14}$$

This way the potentials in both directions are harmonic as expected, and we get the 2D Lissajous lens [5].

III.2. Multi-focal Lissajous lens

We again choose $T_x(E_x) = T = \text{const.}$ and require both potentials U_x, U_y to be symmetric. However, now we no longer set k to be constant thoughout the full range of E_x, but we instead put

$$k = \begin{cases} 2 & \text{for } E_x \le E/2 \\ 1 & \text{for } E_x > E/2\,. \end{cases} \tag{15}$$

The potential U_x is again given by Eq. (14). For $|y| \le T\sqrt{E}/(2\pi)$, the potential U_y is given by Eq. (14) with $k = 1$; for $|y| > T\sqrt{E}/(2\pi)$, it can be found by inverting the relation $\Delta y(U_y) = T[(\sqrt{U_y} + \sqrt{U_y - E/2})/(\pi\sqrt{2})$. The resulting potential U_y is shown in Fig. 1 (a) and the trajectories are in Fig. 1 (b). As we see, there are two classes of trajectories. For the first class in which $E_x \le E/2$, the particle motion is confined to the region $|y| \le T\sqrt{E}/(2\pi)$ with the 2D Hooke potential; the trajectories are therefore concentric ellipses. For the second class with $E_x > E/2$, the particle gets outside this region, the trajectories are still closed, but now it takes two oscillations in the x direction per one oscillation in the y direction. In the optical case, we get this way a multi-focal lens in a similar way as in [9].

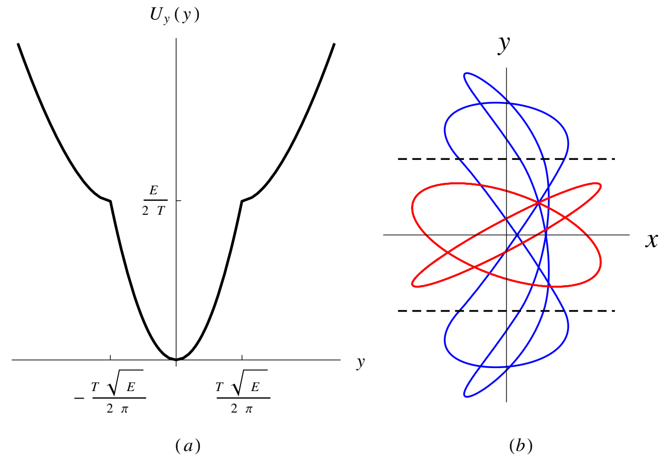

FIG. 1. (a) Potential $U_y(y)$ and (b) Ray trajectories in the refractive index profile for a multi-focal Lissajous lens. The rays corresponding to $k = 1$ are shown in red while those corresponding to $k = 2$ are shown in blue. The boundaries $y = \pm T\sqrt{E}/2\pi$ are shown by the dashed lines.

III.3. Infinite well in the x-direction

Let us choose $U_x(x)$ as a potential of an infinite square well of width a:

$$U_x(x) = \begin{cases} 0 & \text{if } |x| \le a/2 \\ \to \infty & \text{otherwise} \end{cases} \tag{16}$$

This in the optical case corresponds to a pair of mirrors placed along the straight lines $x = \pm a/2$. Substituting $U_x(x)$ above into Eq. (13) gives

$$\begin{aligned} \Delta y(U_y) &= \frac{2k}{\pi}\int_{-a/2}^{a/2} \ln\left[\frac{\sqrt{U_y} + \sqrt{E}}{\sqrt{E - U_y}}\right] \mathrm{d}x \\ &= \frac{2ka}{\pi} \ln\left[\frac{\sqrt{U_y} + \sqrt{E}}{\sqrt{E - U_y}}\right]\,. \end{aligned} \tag{17}$$

If we require a symmetric U_y and invert Eq. (17), we get

$$U_y = E\left[1 - \frac{1}{\cosh^2 \frac{\pi y}{ka}}\right]\,. \tag{18}$$

The corresponding refractive index profile is

$$n = \frac{\sqrt{2E}}{\cosh \frac{\pi y}{ka}}\,. \tag{19}$$

This is the well-known profile of the Mikaelian's self-focusing lens [10]. The ray trajectories in this index profile (combined with the mirrors at $x = \pm a/2$) are plotted in Fig. 2 for two values of k.

III.4. Optical conformal mapping leading to radially symmetric absolute instruments

It is obvious from the construction of the lens in the previous example as well as from Fig. 2 that if the ver-

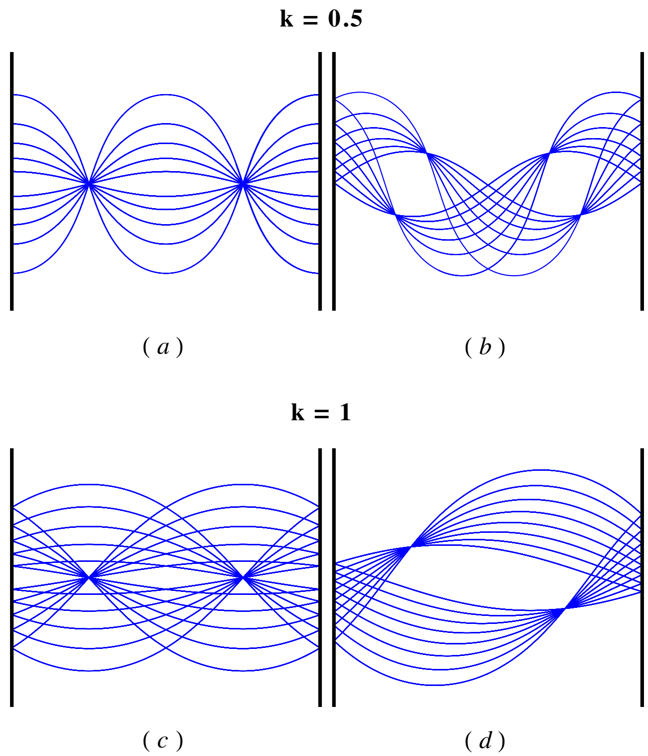

FIG. 2. Ray trajectories in the infinite potential x-well corresponding to the refractive index profile in Eq. (19) for two values of k.

tical mirrors were absent and the potential $U_x(x) = 0$ were extended periodically on either side, that rays would form curves that would be periodic in x. The coordinate system and motion would then be infinite and open, respectively. We can, however, identify the lines $x = -a/2$ and $x = a/2$ with one another, to effectively wrap the xy plane into a cylinder. We will further assume that $a = 2\pi$ and employ optical conformal mapping [12, 13] using the exponential function $\mathrm{e}^{y+\mathrm{i}x} = r\mathrm{e}^{\mathrm{i}\varphi}$ from the original plane (cylinder) xy (now to be called virtual space) to a new plane with polar coordinates r, φ (to be called physical space). This transforms the refractive index profile (19) of virtual space into a new profile in physical space

$$n = \frac{\sqrt{2E}}{r(r^{1/2k} + r^{-1/2k})} \tag{20}$$

that depends only on the radial coordinate. Eq. (20) describes the generalized Maxwell fish eye lens [2, 14] and in the particular case of $k = 1/2$ it corresponds to the Maxwell fish eye profile [3].

Moreover, if we in Sec. III.3 relax the requirement of symmetry of the potential U_y, the above described optical conformal mapping method would generate a much broader class of AIs. In particular, one can show that the freedom discussed below Eq. (6) would give the 2D versions of all the absolute instruments obtained by the very general method described in Ref. [2]. This way, by adjusting k and $y_1(U_y)$ in a suitable way one can obtain the Luneburg lens, Eaton lens, Miñano lens and all other lenses with radial symmetry.

III.5. Lens with an angular dependence of refractive index

In the last example we will extend the ideas from the previous section. To do so, we will again identify the lines $x = -a/2$ and $x = a/2$, transforming the plane xy into a cylinder, but this time we will no longer assume that the potential U_x is constant, but instead we take it as the harmonic potential

$$U_x(x) = \frac{1}{2}\left(\frac{2\pi}{T}\right)^2 x^2 \,. \tag{21}$$

Now there will be two types of trajectories. Particles with energies E_x less than the maximum $U_x(a/2)$ will be confined by a local potential well and will follow Lissajous-like trajectories with the choice of an appropriate accompanying U_y. Particles with energies E_x greater than the maximum $U_x(a/2)$ will not be confined by the potential well in the x direction; they will reach the point $x = \pm a/2$ and go around the cylinder. We see that thanks to the cylindrical topology of the configuration space, the motion even of these particles is periodic. We can then calculate U_y with the help of Eq. (13) to get

$$\Delta y(U_y) = \frac{4}{\pi k}\int_0^{a/2} \ln\left(\frac{\sqrt{U_y} + \sqrt{E - \frac{1}{2}\left(\frac{2\pi}{T}\right)^2 x^2}}{\sqrt{E - U_y - \frac{1}{2}\left(\frac{2\pi}{T}\right)^2 x^2}}\right) \mathrm{d}x \,. \tag{22}$$

Then, again by conformally mapping the corresponding Cartesian refractive index profile into polar coordinates of physical space, $\mathrm{e}^{y+\mathrm{i}x} = r\mathrm{e}^{\mathrm{i}\varphi}$, we obtain an absolute optical instrument with two classes of closed rays: the rays in one class orbit the origin, and the rays in the second class do not. Ray trajectories corresponding to the symmetric choice of $U_y(y)$ are shown in Fig. 3 for $k = 1$ and $E = \pi^2$.

IV. 3D ABSOLUTE INSTRUMENTS

Let us now extend our method to three dimensions. Consider a Lagrangian that separates in Cartesian coordinates x, y, z. Similarly as in 2D, each spatial direction will have its energy conserved and all af these energies sum to the total energy $E = E_x + E_y + E_z$. Now to get an absolute instrument, we have to keep the ratios of the three periods of motion T_x, T_y and T_z rational for any allowed combination of E_x, E_y and E_z. Imagine for a moment that we keep E_z fixed and vary E_x and E_y only. As a consequence, T_z remains fixed, and therefore also T_x and T_y must be fixed to keep the ratios T_x/T_z and T_y/T_z rational. Therefore the potentials U_x and U_y must be such that their oscillation periods do not depend on the energy, and by the same argument this holds also

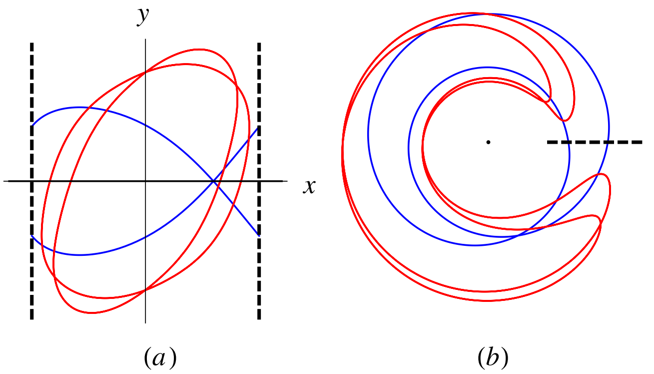

FIG. 3. Ray trajectories in the refractive index profile corresponding to the potential described in Section III.5 with (a) periodicity in the y-direction between the horizontal lines, and (b) a lens formed by a conformal map where y is mapped to the polar coordinate. The dashed lines in both figures are spatially equivalent in the conformal map, and the two classes of rays described in the text are indicated by different colors.

for $U_z(z)$. An obvious case when this is satisfied is that the potentials U_x, U_y and U_z are harmonic, so the total potential $U = U_x + U_y + U_z$ corresponds to a (generally anisotropic) harmonic oscillator in three dimensions. In the optical case, this corresponds to the Lissajous lens [5]. However, this is not the only case because there is still the freedom discussed below Eq. (6), so for each potential U_x, U_y and U_z there are infinitely many options.

For example, we can choose $T_x(E_x) = T = \text{const.}$, $T_y(E_y) = k_1 T$, and $T_z(E_z) = k_2 T$, and then require that potentials U_x and U_z be symmetric, but allow U_y to be asymmetric in a way that preserves the required properties of the potential. We get from Eq. (6) $\Delta x(U_x) = 2T\sqrt{U}_x/(\pi\sqrt{2})$, $\Delta y(U_y) = 2k_1 T\sqrt{U}_y/(\pi\sqrt{2})$, and $\Delta z(U_z) = 2k_2 T\sqrt{U}_z/(\pi\sqrt{2})$, and with the freedom discussed we can choose the following potential where α is a real number ($0 < \alpha < 2$):

$$U_x(x) = \frac{1}{2}\left(\frac{2\pi}{T}\right)^2 x^2\,, \qquad U_z(z) = \frac{1}{2}\left(\frac{2\pi}{k_2 T}\right)^2 z^2\,,$$

$$U_y(y) = \begin{cases} \frac{1}{2}\left(\frac{2\pi}{\alpha k_1 T}\right)^2 y^2 & \text{if } y \geq 0 \\ \frac{1}{2}\left(\frac{2\pi}{(\alpha-2) k_1 T}\right)^2 y^2 & \text{otherwise}\,. \end{cases} \tag{23}$$

This particular function $U_y(y)$ was chosen so that the inversion of $\Delta y(U_y)$ would be analytic and compact, but an infinite number of other functions would also work. Ray trajectories for two choices of α are shown in Fig. 4, with $k_1 = 2$, $k_2 = 1$, $T = 2\pi$, and $E = 1$.

Making use of the asymmetry thus gives a plethora of new 3D absolute instruments. We have to say, however, that compared to the 2D case, in 3D we do not have the freedom of choosing the periods as functions of energy that has been employed in Sec. II.1, and the periods for the motion in each direction must be constant. Therefore the set of asymmetric absolute instruments in 3D is much less rich compared to the 2D case.

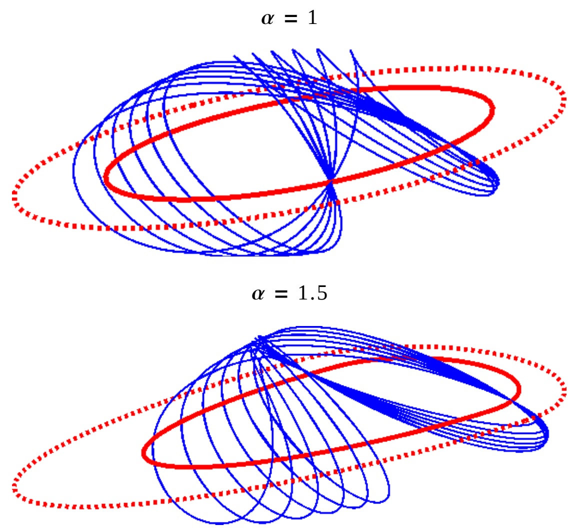

FIG. 4. Ray trajectories in the three-dimensional potential in Eq. (23) for two values of α. The solid and dotted red curves respectively show where the index of refraction are unity and zero, on the xy plane in each figure. When $\alpha = 1$, the ray trajectories are Lissajous curves.

V. CONCLUSION

In conclusion, we have presented a method for constructing the refractive indices for absolute optical instruments without spherical symmetry. This method allows construction of lenses where the Lagrangian of the corresponding mechanical problem is separable in the Cartesian coordinate system. For 2D lenses, the method allows a huge design space and greatly encompasses the known number of AIs. In 3D, our method still gives an uncountable number of absolute instruments; however, their set is much more limited than in the 2D case.

In this paper we have examined only cases where the Lagrangian is separable in the Cartesian coordinate system. We have not examined the cases of separation in other coordinate systems. This could give other, still unknown abslolute instruments, which is a subject of further investigation.

VI. ACKNOWLEDGMENTS

T. Tyc acknowledges support of the grant P201/12/G028 of the Czech Science Foundation, and of the QUEST program grant of the Engineering and Physical Sciences Research Council. H. L. Dao acknowledges grant NRF-CRP 4-2008-06 from National Research Foundation - Prime Ministers Office, Singapore.

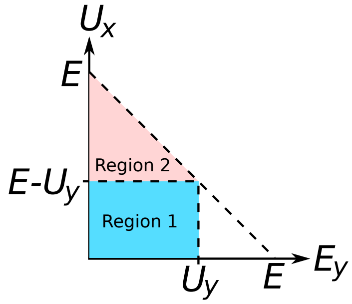

FIG. 5. Integration regions for the transformation of integrals in Eq. (24).

APPENDIX

The double integral in Eq. (11) corresponds to the integration region in the plane (E_y, U_x) consisting of two parts, Regions 1 and 2, shown in Fig. 5. To evaluate it, we interchange the order of integration in each region, changing the limits appropriately:

$$\int_0^{U_y} \mathrm{d}E_y \int_0^{E-E_y} \mathrm{d}U_x = \int_0^{E-U_y} \mathrm{d}U_x \int_0^{U_y} \mathrm{d}E_y + \int_{E-U_y}^{E} \mathrm{d}U_x \int_0^{E-U_x} \mathrm{d}E_y \tag{24}$$

Then Eq. (11) becomes

$$\Delta y(U_y) = \frac{k}{\pi}\int_0^{E-U_y} \frac{\mathrm{d}\Delta x}{\mathrm{d}U_x}\, I_1(U_x,U_y)\,\mathrm{d}U_x + \frac{k}{\pi}\int_{E-U_y}^{E} \frac{\mathrm{d}\Delta x}{\mathrm{d}U_x}\, I_2(U_x,U_y)\,\mathrm{d}U_x\,, \tag{25}$$

where we have denoted the integrals

$$I_1(U_x,U_y) = \int_0^{U_y} \frac{\mathrm{d}E_y}{\sqrt{E-E_y-U_x}\sqrt{U_y-E_y}}\,, \tag{26}$$

$$I_2(U_x,U_y) = \int_0^{E-U_x} \frac{\mathrm{d}E_y}{\sqrt{E-E_y-U_x}\sqrt{U_y-E_y}}\,. \tag{27}$$

These integrals can be readily evaluated using the indefinite integral

$$\int \frac{\mathrm{d}E_y}{\sqrt{E-E_y-U_x}\sqrt{U_y-E_y}} = \tag{28}$$

$$-2\ln\left[\sqrt{E-E_y-U_x}+\sqrt{U_y-E_y}\right]\,, \tag{29}$$

which yields

$$I_1 = 2\ln\frac{\sqrt{U_y}+\sqrt{E-U_x}}{\sqrt{E-U_x-U_y}}\,, \tag{30}$$

$$I_2 = 2\ln\frac{\sqrt{U_y}+\sqrt{E-U_x}}{\sqrt{U_x+U_y-E}}\,. \tag{31}$$

Taking into account that in each respective region (Region 1 for I_1 and Region 2 for I_2) the expression in the square root in the denominator is non-negative, we can replace these terms in both expressions simply by $|E-U_x-U_y|$. Substituting then Eqs. (30) and (31) into Eq. (25), we finally get Eq. (12).

VII. REFERENCES AND FOOTNOTES

[1] M. Born and E. Wolf, *Principles of Optics* (Cambridge University, 2006)
[2] T. Tyc, L. Herzánová, M. Šarbort, and K. Bering, "Absolute instruments and perfect imaging in geometrical optics," New J. Phys. **13**, 115004 (2011)
[3] Maxwell J C 1854 Camb. Dublin Math. J. 8 188
[4] J. C. Miñano, "Perfect imaging in a homogeneous three-dimensional region," Opt. Express **14**, 9627-9635 (2006)
[5] A. J. Danner, H. L. Dao, T. Tyc, "The Lissajous lens: a three-dimensional absolute optical instrument without spherical symmetry" Opt. Express **23**, 5716-5722 (2015)
[6] U. Leonhardt and T. Philbin, *Geometry and light: The science of invisibility* (Dover, Mineola, 2010)
[7] L. D. Landau and E. M. Lifschitz, *Mechanics* (Pergamon Press, 1969)
[8] M. Šarbort and T. Tyc, "Spherical media and geodesic lenses in geometrical optics," J. Opt. **14**, 075705 (2012)
[9] M. Šarbort and T. Tyc, "Multi-focal spherical media and geodesic lenses in geometrical optics," J. Opt. **15**, 125716 (2013)
[10] A. L. Mikaelian, "Self-focusing media with variable index of refraction", Progress in Optics XVII, 283 (1980).
[11] J. M. Jauch and E. L. Hill, "On the problem of degeneracy in quantum mechanics", Phys. Rev., **57**, 641-645 (1940)
[12] U. Leonhardt, "Optical conformal mapping," Science **312**, 1777-1780 (2006)
[13] L. Xu and H. Y. Chen, "Conformal Transformation Optics", Nature Photon., **9**, 15-23 (2015)
[14] Y. N. Demkov and V. N. Ostrovsky, "Internal symmetry of Maxwell fish-eye problem and Fock group for hydrogen atom", Sov. Phys.-JETP **33**, 1083 (1971)
[15] J. B. Pendry, D. Schurig, and D. R. Smith, "Controlling electromagnetic fields," Science **312**, 1780-1782 (2006)
[16] U. Leonhardt and T. Tyc, "Broadband invisibility by non-Euclidean cloaking," Science **323**, 110-112 (2009)
[17] R. K. Luneburg, *Mathematical theory of optics* (University of California, 1964).
[18] T. Tyc and A. J. Danner, "Frequency spectra of absolute optical instruments," New J. Phys. **14**, 085023 (2012)

[19] T. Tyc, “Spectra of absolute instruments from the WKB approximation,” New J. Phys. **15**, 065005 (2013)
[20] H. Goldstein, C. Poole, and J. Safko, *Classical mechanics* (Addison-Wesley, 2001)